University of Zurich[UZH]

Zurich Open Repository and Archive
University of Zurich
University Library
Strickhofstrasse 39
CH-8057 Zurich
www.zora.uzh.ch

Year: 2018

Oxidative stress and altered mitochondrial protein expression in the absence of amyloid- and tau pathology in iPSC-derived neurons from sporadic Alzheimer's disease patients

Birnbaum, Julian H ; Wanner, Debora ; Gietl, Anton F ; Saake, Antje ; Kündig, Thomas M ; Hock, Christoph ; Nitsch, Roger M ; Tackenberg, Christian

Abstract: Mitochondrial dysfunction is a prominent feature of Alzheimer's disease (AD) and increased production of reactive oxygen species (ROS) has been described in postmortem brain samples and animal models. However, these observations were made at a late stage of disease and the inability to examine an early, presymptomatic phase in human neurons impeded our understanding of cause or consequence of mitochondrial dysfunction in AD. We used human induced pluripotent stem cell-derived neuronal cells (iN cells) from sporadic AD (SAD) patients and healthy control subjects (HCS) to show aberrant mitochondrial function in patient-derived cells. We observed that neuronal cultures from some patients produced more ROS and displayed higher levels of DNA damage. Furthermore, patient-derived cells showed increased levels of oxidative phosphorylation chain complexes, whereas mitochondrial fission and fusion proteins were not affected. Surprisingly, these effects neither correlated with A nor phosphorylated and total tau levels. Synaptic protein levels were also unaffected in SAD iN cells. The results of this study give new insights into constitutional metabolic changes in neurons from subjects prone to develop Alzheimer's pathology. They suggest that increased ROS production may have an integral role in the development of sporadic AD prior to the appearance of amyloid and tau pathology.

DOI: https://doi.org/10.1016/j.scr.2018.01.019

Posted at the Zurich Open Repository and Archive, University of Zurich
ZORA URL: https://doi.org/10.5167/uzh-160879
Journal Article
Published Version

The following work is licensed under a Creative Commons: Attribution-NonCommercial-NoDerivatives 4.0 International (CC BY-NC-ND 4.0) License.

Originally published at:
Birnbaum, Julian H; Wanner, Debora; Gietl, Anton F; Saake, Antje; Kündig, Thomas M; Hock, Christoph; Nitsch, Roger M; Tackenberg, Christian (2018). Oxidative stress and altered mitochondrial protein expression in the absence of amyloid- and tau pathology in iPSC-derived neurons from sporadic Alzheimer's disease patients. Stem Cell Research, 27:121-130.
DOI: https://doi.org/10.1016/j.scr.2018.01.019

Stem Cell Research 27 (2018) 121–130

Contents lists available at ScienceDirect

Stem Cell Research

journal homepage: www.elsevier.com/locate/scr

Oxidative stress and altered mitochondrial protein expression in the absence of amyloid-β and tau pathology in iPSC-derived neurons from sporadic Alzheimer's disease patients

Julian H. Birnbaum [a,b], Debora Wanner [a], Anton F. Gietl [a], Antje Saake [a], Thomas M. Kündig [c], Christoph Hock [a], Roger M. Nitsch [a,b], Christian Tackenberg [a,b,*]

[a] University of Zurich, Institute for Regenerative Medicine, Schlieren, Switzerland
[b] University of Zurich, Neuroscience Center Zurich, Zurich, Switzerland
[c] Department of Dermatology, University Hospital Zurich, Zurich, Switzerland

ARTICLE INFO

Article history:
Received 22 November 2017
Received in revised form 15 January 2018
Accepted 17 January 2018
Available online 28 January 2018

Keywords:
Alzheimer's disease
Induced pluripotent stem cells
Induced neuronal cells
Sporadic AD
Mitochondria
Aβ

ABSTRACT

Mitochondrial dysfunction is a prominent feature of Alzheimer's disease (AD) and increased production of reactive oxygen species (ROS) has been described in postmortem brain samples and animal models. However, these observations were made at a late stage of disease and the inability to examine an early, presymptomatic phase in human neurons impeded our understanding of cause or consequence of mitochondrial dysfunction in AD. We used human induced pluripotent stem cell-derived neuronal cells (iN cells) from sporadic AD (SAD) patients and healthy control subjects (HCS) to show aberrant mitochondrial function in patient-derived cells. We observed that neuronal cultures from some patients produced more ROS and displayed higher levels of DNA damage. Furthermore, patient-derived cells showed increased levels of oxidative phosphorylation chain complexes, whereas mitochondrial fission and fusion proteins were not affected. Surprisingly, these effects neither correlated with Aβ nor phosphorylated and total tau levels. Synaptic protein levels were also unaffected in SAD iN cells. The results of this study give new insights into constitutional metabolic changes in neurons from subjects prone to develop Alzheimer's pathology. They suggest that increased ROS production may have an integral role in the development of sporadic AD prior to the appearance of amyloid and tau pathology.

© 2018 The Authors. Published by Elsevier B.V. This is an open access article under the CC BY-NC-ND license (http://creativecommons.org/licenses/by-nc-nd/4.0/).

1. Introduction

Alzheimer's disease is the most prevalent neurodegenerative disease and characterized by the appearance of amyloid-plaques and neurofibrillary tangles in the human brain (Winblad et al., 2016). AD is classified in an early-onset, familial type (FAD) and a late-onset, sporadic type, which represents about 95% of the cases (Winblad et al., 2016). The cause for FAD are mutations in APP, PSEN1 or PSEN2, whereas the underlying mechanisms in SAD are still not clear. Genome-wide association studies (GWAS) have identified a single nucleotide polymorphisms (SNPs) for SAD risk but provided little information about biological processes (Nicolas et al., 2016). Further, dysregulation of an entire pathway can be caused by mutations dispersed throughout the genome, yet these might not be identified due to their different locations. Induced pluripotent stem cells (iPSCs) offer a new venue to AD research, not only due to the ability to model sporadic diseases but also because they allow the use of human cells. Thus far, multiple studies used iPSC-derived neurons to assess AD pathology and possible treatments. Drug testing was applied to elucidate mechanisms of APP processing (Brownjohn et al., 2017; Mertens et al., 2013) and several groups used iPSCs with familial AD mutations to show increased Aβ production and tau phosphorylation (Moore et al., 2015; Woodruff et al., 2013; Yagi et al., 2011) caused by these mutations. Two of the first studies using AD patient-derived neuronal cells were comparing SAD to FAD-derived cells (Kondo et al., 2013; Israel et al., 2012). Israel and colleagues used lines from two patients with APP duplications and two SAD patients with one SAD line behaving like non-demented controls and the second line similar to FAD lines, in regard to Aβ production, p-tau and active GSK-3-β levels. Kondo et al. used two different familial mutations and SAD patient cells. APP-E693Δ and one SAD line showed higher ROS levels and intracellular Aβ.

Mitochondrial dysfunction such as increased oxidative mtDNA damage (Hirai et al., 2001; Mecocci et al., 1994) or higher cytochrome oxidase levels (Hirai et al., 2001; Nagy et al., 1999) have been hypothesized to be the potential causes of oxidative stress in AD brains.

Abbreviations: AD, Alzheimer's disease; CSF, cerebrospinal fluid; FAD, familial Alzheimer's disease; GWAS, genome-wide association study; HCS, healthy control subject;; iN cell, induced neuronal cell; iPSC, induced pluripotent stem cell; Oxphos, oxidative phosphorylation chain; PiB, Pittsburgh compound B; SAD, sporadic Alzheimer's disease; ROS, reactive oxygen species.

* Corresponding author.
E-mail address: christian.tackenberg@irem.uzh.ch (C. Tackenberg).

https://doi.org/10.1016/j.scr.2018.01.019
1873-5061/© 2018 The Author(s). Published by Elsevier B.V. This is an open access article under the CC BY-NC-ND license (http://creativecommons.org/licenses/by-nc-nd/4.0/).

Also, an increase of mitochondrial fission protein Fis1 with concurrent downregulation of Drp1 and fusion proteins Mfn1/2 and OPA1 has been reported (Wang et al., 2009). In mouse models of familial AD reduced oxidative and complex I activity has been found (Derungs et al., 2017; Rhein et al., 2009; Trushina et al., 2012), as well as impaired complex III and IV activity (Rhein et al., 2009; Caspersen et al., 2005). Whereas a contradicting report found higher mRNA levels of complex I, III, IV and V in the cortex of Tg2576 mice (Reddy et al., 2004). Observations in triple transgenic mice showed increased oxidative stress levels prior to plaque deposition (Yao et al., 2009). In conclusion, mitochondrial dynamics and function are affected in AD, yet it remains difficult to delineate a clear mechanism due to a lack of human material to examine an early time point of the disease and because findings in mouse models might be affected by overexpression artifacts (Saito et al., 2014; Saito et al., 2016).

Where prior studies focused on Aβ-mediated pathology, we aimed to examine mitochondrial dysfunction at an early stage of disease. In this study we show that iPSC-derived induced neuronal cells from SAD patients show in part increased ROS production and display higher levels of oxidative phosphorylation chain (oxphos) complexes. These effects did not correlate with Aβ and tau levels.

2. Materials and methods

2.1. Culture and reprogramming of human fibroblasts

Fibroblasts were obtained from skin biopsies. Samples were reduced to small pieces and plated in hFib medium (DMEM (ThermoFisher Scientific) + 10% FCS + 2 ng/ml bFGF (Peprotech)). Fibroblasts were split by trypsination and transduced with reprogramming plasmids at passage 3 (P3). A total of 1 μg of plasmids pCXLE-hUL, pCXLE-hSK and pCXLE-hOCT3/4-shp53-F (Addgene: 27,080, 27,078, 27,077) (Okita et al., 2011) were delivered by nucleofection with the Neon transfection system (ThermoFisher Scientific) to 10^5 cells using the following settings: 950 V, 40 ms, 2×. Cells were plated in hFib medium supplemented with 0.1 μM sodium butyrate (Sigma). Medium was changed every other day. On day 7 cells were replated on growth factor reduced matrigel (200 μg/ml, Corning) in hFib medium + 0.1 μM sodium butyrate + 2 μM Thiazovivin(Sigma). Next day medium was changed to E7 (Stemcell Technologies) (Chen et al., 2011) +0.1 μM sodium butyrate and changed every other day until d21. iPSC colonies were picked under a stereomicroscope and expanded in E8 medium (ThermoFisher Scientific) (Chen et al., 2011). Ten colonies of each patient and control subject were picked and characterized (see Fig. 1 and Fig. S1) and two of these colonies (clones) were used for subsequent experiments to account for clonal variation. Main figures show the data of two clones pooled to represent the changes in a patient or control subject. Data for individual clones are displayed in the supplementary figures.

2.2. Maintenance of iPSCs

IPSCs were maintained in E8-flex medium (ThermoFisher Scientific) on growth factor reduced matrigel (Corning). Cells were split once to twice a week with ReLeSR (StemCell Technologies), according to manual. All iPSC lines were tested negative for mycoplasma.

2.3. Differentiation of iPSCs to iN cells

Cells were differentiated according to Zhang et al. (Zhang et al., 2013), with slight modifications. On day −2 iPSCs were dissociated with Accutase (ThermoScientific) and 9–20 × 10^4 cells (depending survival of the cell line) plated on matrigel coated coverslips in a 24-well plate in E8 supplemented with Thiazovivin (2 μM, Sigma). Cells were infected with lentiviruses expressing rtTA and Neurogenin2 on day −1 in fresh E8 medium. On day 0 medium was changed to induction medium (DMEM/F12 (ThermoScientific) with doxycyclin (2 μg/ml), 1× N2 (ThermoFisher), 1× NEAA (Sigma), BDNF (10 ng/ml, Peprotech), NT-3 (10 ng/ml, Peprotech) and Laminin (200 μg/ml, Sigma)). On day 1, induction medium was changed and supplemented with Puromycin (1 μg/ml, Sigma) for a 24 h selection period. On day 2, 70.000 glia cells were added in iN-Neurobasal medium (Neurobasal-A (ThermoFisher) with 1× B27 (Gibco), 2 mM Glutamax (Gibco), 2 μM AraC (Sigma), 2 μg/ml Doxycyclin, 10 ng/ml BDNF, 10 ng/ml NT-3, and 200 μg/ml Laminin)). 50% of the medium was changed every other day until day 10, when medium was changed to Neuronal medium (MEM (ThermoFisher), 1× B27, 0.5% Glucose, 0.02% $NaHCO_3$, 100 μg/ml Transferrin (Sigma), 5% FCS, 0.5 mM L-glutamine and 2 μM AraC). Neuronal medium was changed twice a week until cells were assayed on day 21–day 23.

2.4. Glia preparation and maintenance

Glia cells were prepared from P1 wild-type CD1 pups as followed. Brain was extracted, meninges removed and forebrain isolated. Forebrains were digested in 10 U/ml papain for 30 min and cells dissociated by pipetting. Cells were plated in DMEM with 10% FCS in t75 flasks. Glia were split 1:3 with trypsin at 80% confluence. Glia was used for co-cultures between passages 2–4.

2.5. Lentiviral production

HEK293T cells were maintained in DMEM with 10% FCS and split every other day by trypsination. Lentiviral vectors including three helper plasmids were delivered by calcium phosphate transfection (Chen & Okayama, 1987). In brief, 5 × 10^7 cells per 15 cm dish were plated for transfection. 12.5 μg VSV-G, 25 μg pMDLg/pRRE, 12.5 μg pREV and 50 μg plasmid of interest were mixed with 625 μl 0.5 M $CaCl_2$ and 625 μl H_2O. Mixture was added dropwise to 1250 μl 2× HBS on a vortexer, incubated for 30 mins at RT and added to cells. Medium was changed the next morning and supernatant harvested after 48 h. Lentivirus was concentrated by centrifugation (25,000 g for 90 min), resuspended overnight in 200 μl E8 and snap frozen in liquid nitrogen. 0.2 μl lentiviral solution were used per 24-well. Lentivirus was produced from the following plasmids: TetO-Ngn2-P2A-puromycin, rtTA, TetO-EGFP, and synapsin-NLS-mCherry. All plasmids were a generous gift from Prof. Thomas C. Südhof, Stanford University.

2.6. ROS assay

To increase cellular stress, iN cells were cultured in the absence of B27 for 3 days prior to the experiment. On DIV21 cells were treated with 5 μM CellRox green reagent (ThermoFisher) for 30 min at 37 °C prior to fixation. NeuN staining was carried out as described below and coverslips imaged within 24 h. Fluorescent intensity was analyzed by CellProfiler Software (Carpenter et al., 2006) by measuring 488 nm wavelength intensity in NeuN positive puncta (647 nm).

2.7. Analysis of DNA damage

Medium was changed two days prior to assay. On day 21, positive control was treated with 5 μM Etoposide (Sigma) for 1 h, prior to fixation. NeuN and p-γ-H2AX staining was carried out as described below. Fluorescent intensity was analyzed by CellProfiler Software by measuring 488 nm wavelength intensity in NeuN positive puncta (647 nm).

2.8. Immunofluorescence experiments

IN cells were fixed in 4% paraformaldehyde in PBS for 20 min at RT. Cells were washed 3× for 10 min with PBS and incubated for 1 h in blocking buffer (10% donkey serum, 0.1% Triton X-100 in PBS). Primary antibody was incubated overnight at 4 °C in staining buffer (PBS with 3% goat serum and 0.1% Triton X-100). Subsequently cells were washed 3×

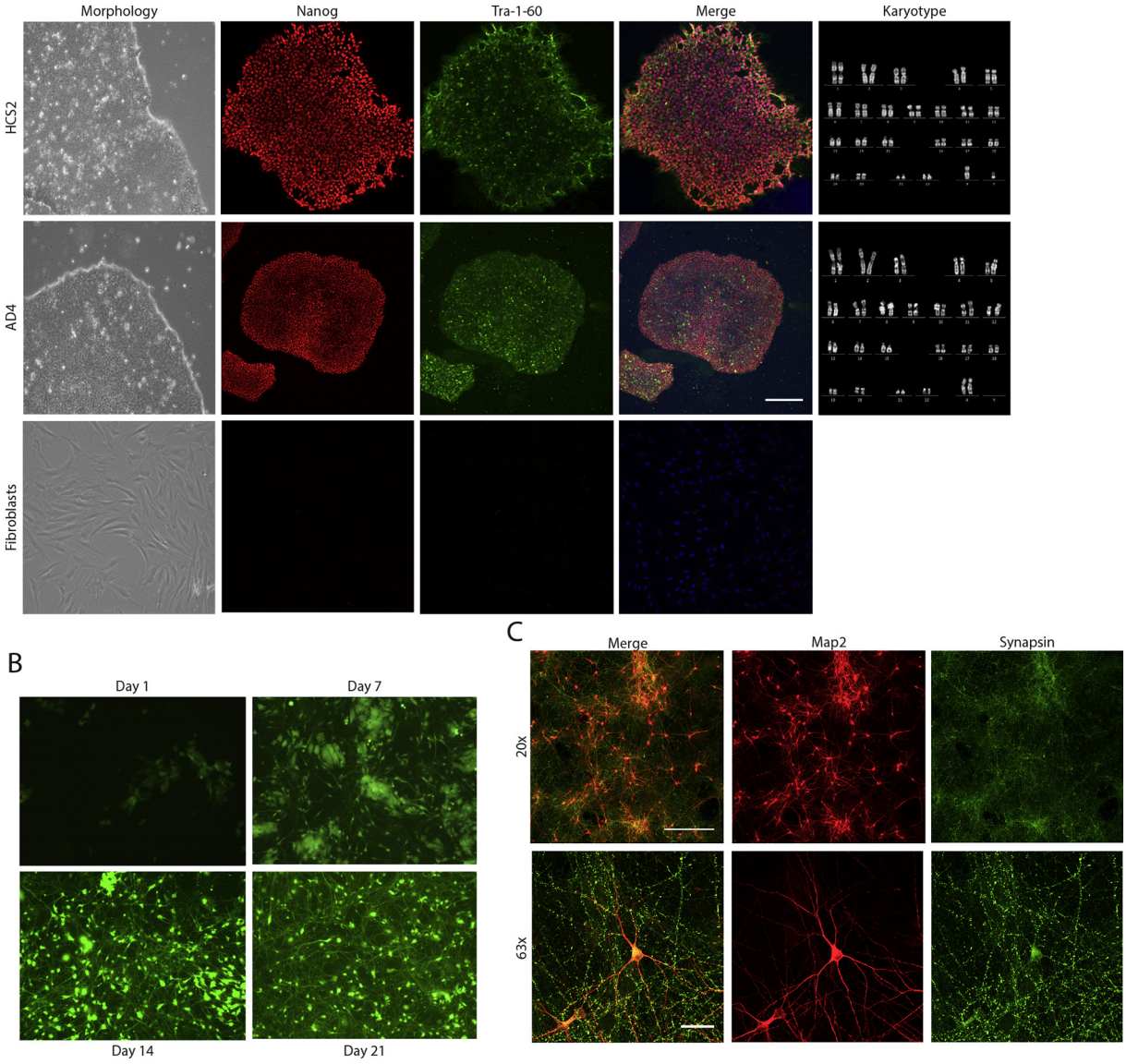

Fig. 1. Fibroblast reprogramming to iPSCs and differentiation to iN cells. A Representative images of one control and one AD patient-derived iPSC line. IPSCs but not fibroblasts showed an embryonic stem cell-like morphology (DIC) and expressed the pluripotency markers Nanog (red) and Tra-1-60 (green). Reprogrammed cells retained a normal karyotype. Scale bar: 300 μm. B Differentiation of iPSCs to iN cells. Overexpression of Ngn2 led to induction of neuronal-like morphology over the course of 21 days, visualized by EPFG expression. Images were taken at 10×. C iN cells at day 21 stained positive for the neuronal marker Map2 (red) and the presynaptic marker synapsin (green). Scale bar: 200 μm (top), 25 μm (bottom).

with PBS and secondary antibody applied in staining buffer for 1.5 h at RT. Cells were washed once and incubated with DAPI for 20 min, then washed 3× and mounted on cover slides. Immunofluorescence was visualized on a Leica SP8 confocal microscope.

Antibodies used:

Primary AB Name	Producer	Cat. No.	Dilution
Anti-Nanog	R&D	Af1997	1:100
Anti-TRA-1-60	Millipore	MAB4360	1:100
Anti-NeuN	Millipore	MAB377	1:100
Anti-Synapsin	Synaptic Systems	106,001	1:500
Anti-Map2	Synaptic Systems	188,003	1:600
Anti-γ-H2AX	Abcam	ab11174	1:500
Secondary AB Name	**Producer**	**Cat. No.**	**Dilution**
Dk-α-ms-Alexa488	Jackson	715–545–151	1:250
Dk-α-rb-Alexa488	Jackson	711–545–152	1:250
Dk-α-gt-cy3	Jackson	705–165–147	1:250
Dk-α-ms-Alexa647	Jackson	715–606-151	1:250
Dk- α-rb-Alexa647	Jackson	711–605–152	1:250

2.9. Immunoblotting and protein quantification

Cells were harvested in RIPA buffer (50 mM Tris-HCl pH 7.6, 150 mM NaCl, 1% NP40, 0.5% SDS, 0.5% sodium deoxycholate, 2 mM EDTA) supplemented with protease inhibitor (Roche) and phosphatase inhibitor cocktail 1 and 3 (Sigma)), snap frozen in liquid nitrogen and stored at −80 °C until use. Lysates were analyzed by SDS-Page on 10–20% Tris-Tricine gels (ThermoFisher Scientific). Immunoblotting was performed using peroxidase conjugated antibodies and detected with an ImageQuant LAS 4000 system (GE Healthcare). Image analysis was carried out in ImageJ. Signals were normalized to β-III-tubulin probed on the same blot. Antibodies used:

Primary AB Name	Producer	Cat. No.	Dilution
Anti-APP (Y188)	Abcam	ab32136	1:1000
Anti-β-III-tubulin	Sigma	T8660	1:500
Anti-Drebrin	Cell Signaling	12,243	1:1000

(continued on next page)

Anti-Drp1 (D6C7)	Cell Signaling	8570S	1:1000
Anti-Phospho-Drp1	Cell Signaling	3455S	1:1000
Anti-Mfn1	Cell Signaling	13196S	1:1000
Anti-Mfn2 (D1E9)	Cell Signaling	11925S	1:1000
Anti-Phospho-Tau (AT8)	ThermoFisher	MN1020	1:500
Anti-PSD-95	Millipore	CP35	1:400
Anti-Synapsin	Synaptic Systems	106,001	1:1000
Anti-Tau	Synaptic Systems	314,004	1:1000
Anti-Total OXPHOS WB Antibody Cocktail	Abcam	ab110413	1:500
Secondary AB Name	Producer	Cat. No.	Dilution
Anti-Mouse ECL IgG	GE Healthcare	NA931–1ML	1:4000
Anti-Rabbit ECL IgG	GE Healthcare	NA934V	1:4000
Anti-Guinea Pig IgG	Jackson	106–035-003	1:4000

2.10. Gene expression analysis

Quantitative RT-PCR was performed to determine mRNA levels of genes of interest. Total RNA was isolated by TRI-Reagent (Sigma). Technical triplicates of each experimental condition were pooled and RNA isolation was carried out according to manufacturer's instructions. DNA was digested by DNaseI (Fermentas). 1 μg RNA was reverse-transcribed to cDNA using the iScript cDNA-synthesis kit (BioRad), according to manual. TaqMan probes with TaqMan Gene Expression Master Mix (ThermoFisher Scientific) were used for expression analysis on a 7900HT Real-Time PCR System (ThermoFisher Scientific). Tubb3 was used as an endogenous control. The assay ID of used TaqMan probes was: human Tubb3, Hs00801390_s1; human GAPDH, Hs02786624_g1; human Fis1, Hs00211420_m1; human Opa1, Hs01047018_m1.

2.11. MSD

Medium of iN cells was conditioned for 7 days and used for analysis. Human Aβ38/40/42 was analyzed with the Aβ Peptide Panel 1 (6E10) Kit (Meso Scale Discovery), according to manufacturer's instructions. Individual values were normalized to neuron numbers determined by dot blot assays probed against β-III-tubulin.

2.12. Karyotyping

Cells were arrested in metaphase by treatment with 80 ng/ml colcemide for 1 h. Harvested and treated with hypotonic solution (0.075 M KCl), followed addition of fix solution (MeOH 3:1 Acetic Acid). Metaphases spreads were stained by Quinacrine (Sigma), imaged on a Zeiss Axioskop HBO 50 fluorescent microscope (Zeiss) and arranged in Ikaros Software (MetaSystems).

2.13. Quantification and statistical analysis

Quantitative data represents means ± SEM. All experiments were independently repeated at least three times (with the exception of the ELISA assay which has been repeated twice). Statistical analyses were conducted with by Prism (GraphPad Software). Statistical comparison between multiple groups were analyzed by d'Agostino-Pearson omnibus normality test and subsequent one-way ANOVA with Tukey's test for normal distributed date or Kruskal-Wallis test with Dunn's multiple comparison post hoc test for non-normal distributed data. Statistical significance was only highlighted between control and patient-derived cells.

2.14. Ethics approval

All performed experiments were conducted with the approval and according to the regulations of the Cantonal Ethics Committee. Dermal punch biopsies were taken following informed consent at the Clinic for Dermatology of the University Hospital Zurich.

2.15. Conflict of interest

The authors declare that they have no conflict of interest.

3. Results

To address the mechanisms of oxidative stress and mitochondrial dysfunction in SAD neuronal cells, we harnessed the iPSC technology (Takahashi et al., 2007) to reprogram AD patient and HCS fibroblasts to pluripotency and differentiated those to induced neuronal cells (iN cells) AD subjects were diagnosed according to standard diagnostic criteria (McKhann et al., 2011), had a documented decline over time, underwent complete clinical work up and neuropsychological testing and had either positive amyloid-PET (11-C-PiB) signal or a typical CSF constellation (Table 1). They were compared to HCSs from the same age group with a negative amyloid-PET.

Fibroblast samples isolated from skin biopsies were reprogrammed in feeder-free conditions (Chen et al., 2011) by delivery of episomal plasmids (Okita et al., 2011). IPSC clones were analyzed for an embryonic stem cell-like morphology, normal karyotype and expression of pluripotency markers Tra-1-60 and Nanog (Fig. 1A and Fig. S1). Two clones per individual, positive for all criteria, were used for subsequent analysis. Neuronal differentiation was carried out by lentiviral delivery of doxycycline-inducible Neurogenin2 (Ngn2) expression (Zhang et al., 2013). Neuronal cells underwent morphological changes over the course of 21 days (Fig. 1B), expressed the neuronal marker Map2, displayed synaptic boutons (Fig. 1C) and showed spontaneous activity in calcium imaging (unpublished results). Cells were co-cultured with mouse glia cells to support survival and synapse formation (Zhang et al., 2013).

Various reports show widespread changes in mitochondrial function in AD. The production of ROS in mitochondria was found to be augmented in AD human samples and mouse models (Mecocci et al., 1994; Yao et al., 2009) and might play an integral role in disease (Grimm et al., 2016). To analyze whether AD patient-derived neurons display higher levels of oxidative stress than HCS neurons we used confocal imaging of CellRox green, a dye that increases fluorescence upon ROS-mediated oxidation. To avoid confounding with glia-derived ROS we measured CellRox intensities in NeuN positive puncta. Menadione treatment was used as a positive control for ROS production. Analysis showed higher ROS levels in AD2, AD3, and AD4 iN cells showing statistical significance compared to both HCS's (Fig. 2A,B). Results of individual clones are shown in Fig. S2. These findings suggested altered mitochondrial function in at least three out of five AD patients.

Table 1
Overview of recruited subjects for this study. Mean age at biopsy was 71.5 (HCS) and 74 (AD) with a range from 63 to 87 years. The individual age is not listed to avoid possible identification of the individuals as requested by the local ethics committee. n.d.: not determined.

	Diagnose	ApoE	PiB-PET SUVR	Biomarker	Gender
HCS1	–	3/3	1.07	n.d.	Male
HCS1	–	3/4	1.17	n.d.	Male
AD1	AD	3/3	n.d.	Aβ: 550 pg/ml P-Tau: 162 pg/ml Total Tau: >1200 pg/ml	Female
AD2	AD	3/4	n.d.	Aβ: 201 pg/ml P- Tau: 160 pg/ml Total Tau: 1094 pg/ml	Female
AD3	AD	3/4	2.4	n.d.	Female
AD4	AD	3/4	2.16	n.d.	Female
AD5	AD	3/3	2.42	n.d.	Female

Increased ROS production may be caused by dysfunctions of the mitochondrial respiratory chain. Assessment of protein levels of oxphos chain subunits are an indicator for altered complex function. Using an oxphos antibody cocktail we showed higher NDUFB8 protein levels, a subunit of oxphos complex I, in AD4 patient cells, compared to both control lines (Fig. 3A,B). We further observed higher protein levels of UQCRC2, a complex III subunit, in cells from AD4 and AD5 compared to HCS1 (Fig. 3A,C). The most striking changes in oxphos chain composition were observed for MTOC1, a complex IV subunit. All AD-derived iN cell lines had higher MTOC1 levels than HCS1, and AD4 and AD5 additionally showed significant higher MTOC1 levels than HCS2 (Fig. 3A, D). Complex V subunit ATP5A showed higher protein amounts in AD2 and AD4 compared to HCS1 (Fig. 3A,E).

Misbalance in mitochondrial dynamics, i.e. fusion and fission, affects mitochondrial integrity and may result in the observed changes in ROS levels (DuBoff et al., 2013). Thus we assessed whether mitochondrial fission and fusion protein levels were altered in AD patient-derived iN cells. Mfn1, Mfn2 and Opa1 regulate mitochondrial fusion. We used western blotting to assess Mfn1 levels but did not observe an alteration in AD-patient iN cells (Fig. 3F,G). Likewise we examined Mfn2 and found no changes in patient cells (Fig. 3F,H). Opa1 mRNA levels, a protein mediating mitochondrial inner membrane fusion, were determined by q-RT-PCR. We found decreased mRNA levels in AD2 cells compared to HCS1, whereas other cell lines showed comparable mRNA levels (Fig. 3I). Regulators of mitochondrial fission are Drp1, its active from phosphorylated-Drp1, and Fis1. We could not observed differences between HCS-derived and patient iN cells in regard to total Drp1 (Fig. 3J, K) and phosphorylated-Drp1 protein levels (Fig. 3J,L). Further, q-RT-PCR of *Fis1* showed similar mRNA levels in control and patient cells (Fig. 3M). Individual clones are depicted in Fig. S3. Examination of mitochondrial function suggests that AD patient-derived iN cells, which are supposed to mimick early changes in AD, are rather affected by altered oxphos complex composition than by defects in mitochondrial dynamics.

Aggregates of Aβ and tau are the major hallmarks of AD and thought to be the main driver of AD pathology. Evidence exists that both, Aβ and tau, affect mitochondrial function and thereby may contribute to ROS generation (Rhein et al., 2009; DuBoff et al., 2013). Therefore we examined whether AD-patient derived iN cells show differences in APP processing, Aβ secretion, as well as tau and phospho-tau levels. We further investigated whether these correlate with the observed misregulation of mitochondrial proteins or increased ROS production in AD patient iN cells. First we assessed levels of APP protein in iN cells from HCS's and AD-patients. As expected from samples of sporadic AD cases, no higher total APP levels could be observed, in fact AD5 APP levels were lower compared to HCS2 (Fig. 4A,B). Amylogenic processing of APP by β-secretase leads to the generation of C99 (β-CTF), whereas α-processing generates C83 (α-CTF). We assessed if ratios and total

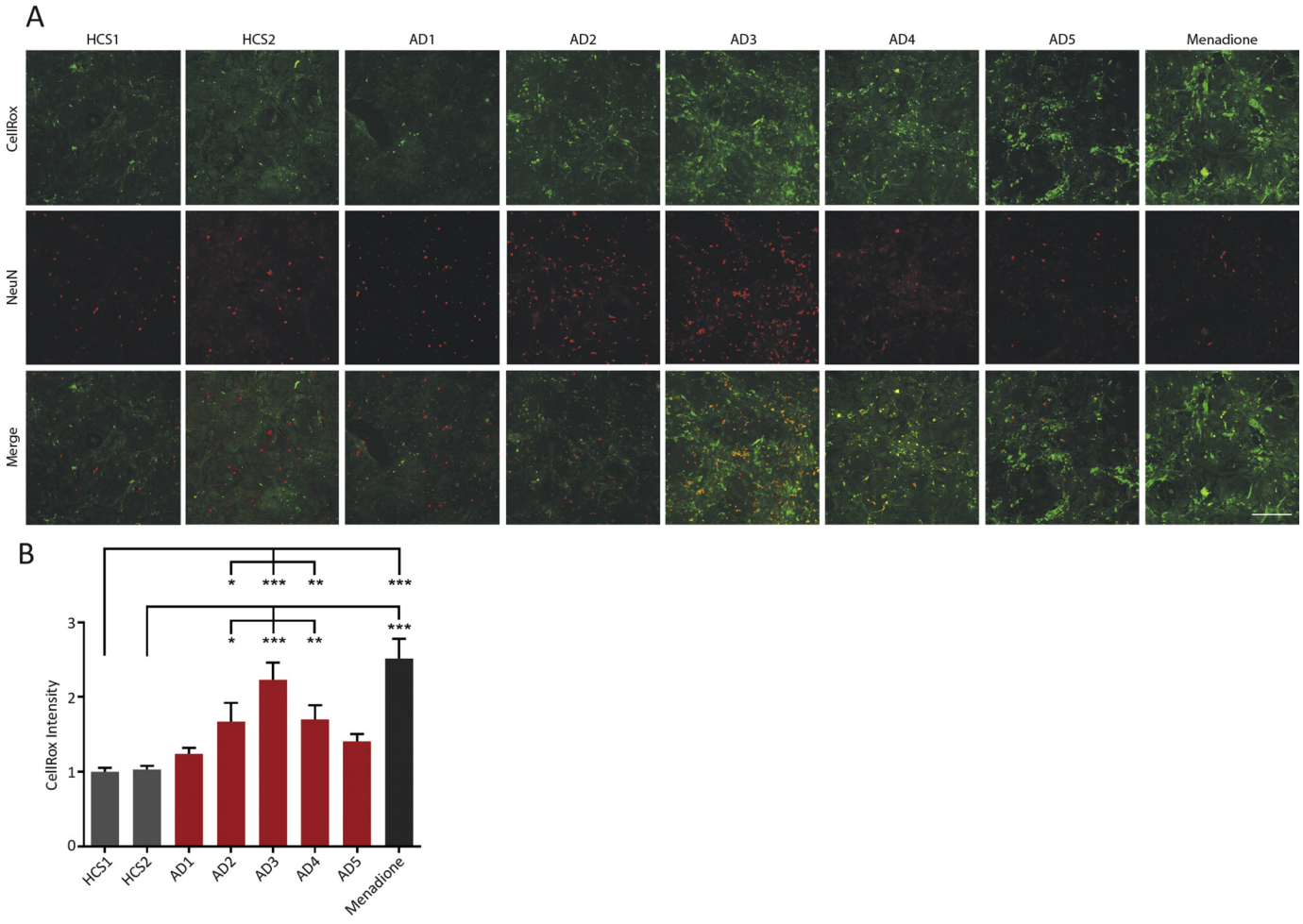

Fig. 2. ROS production in AD patient and HCS iN cells. A Representative confocal images (20×) of iN cells stained with CellRox green dye followed by immunostaining against NeuN. CellRox intensity was assessed in overlay with NeuN positive puncta using Cell Profiler software. Menadione 50 μM was used as positive control. B Quantification of CellRox intensity. ROS production was significantly higher in AD2, AD3,and AD4 iN cells compared to HCS1 and HCS2. Scale bar: 200 μm. Data are means ± SEM (n = 14–22). Statistical significance was assessed by Kruskal-Wallis test (*$p < 0.05$; **$p < 0.01$; ***$p < 0.001$).

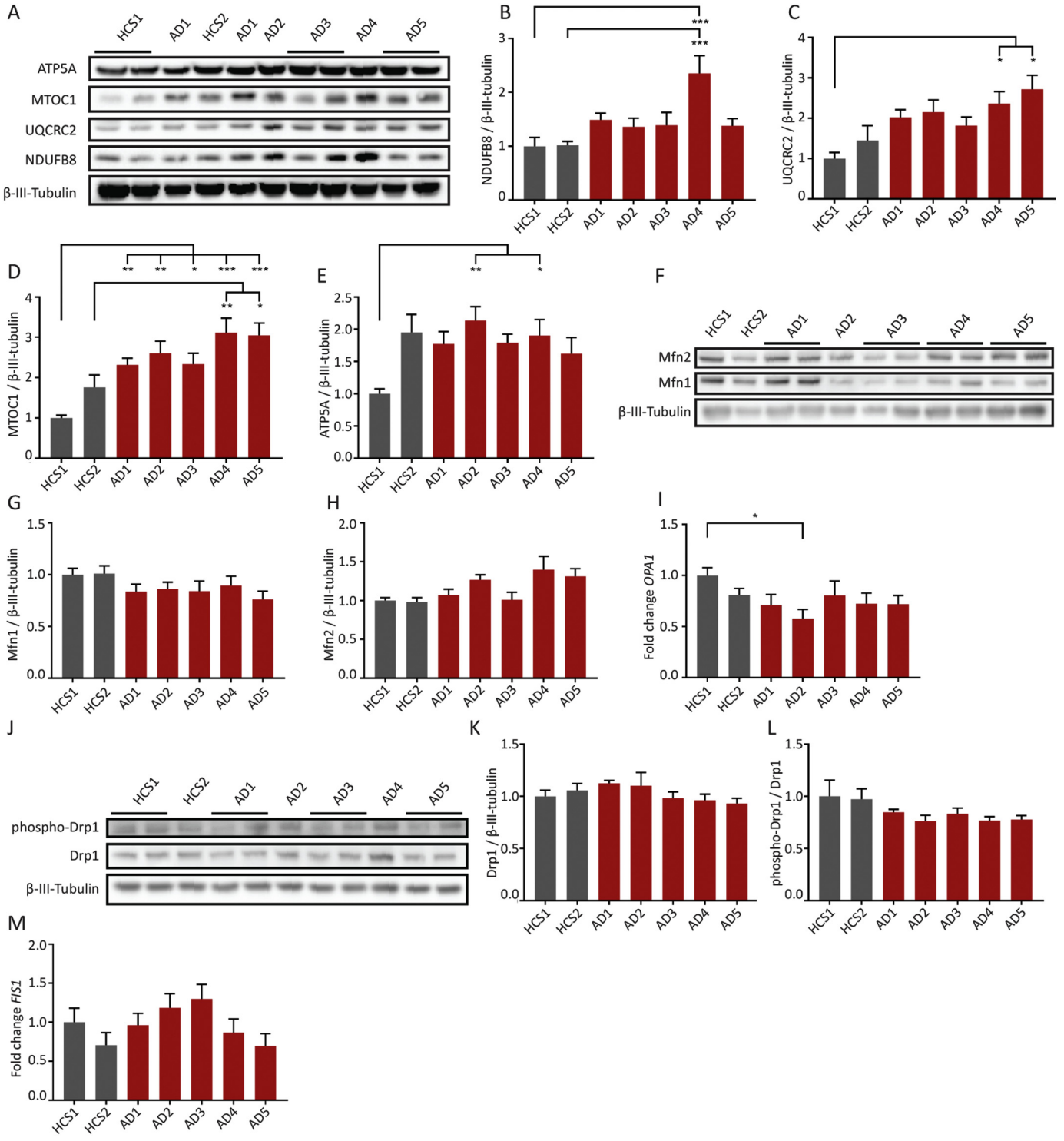

Fig. 3. Levels of mitochondrial proteins and mRNA in iN cells from HCS and AD patients. A Assessment of mitochondrial oxidative phosphorylation chain complex I, III, IV and V subunits by western blot using oxphos antibody cocktail. B Complex I subunit NDUFB8 was elevated in AD4 iN cells. C Complex III subunit UQCRC2 was significantly higher in AD4 and AD5 iN cells compared to HCS1. D MTOC1, a complex IV subunit, was higher in all AD-patient-derived iN cells compared to HCS1 and higher in AD4 and AD5 cells to HCS2. E Complex V subunit ATP5A levels were higher in AD2 and AD4 compared to HCS1. F Mitochondrial fusion proteins Mfn1 and Mfn2 levels were assessed by western blot. G Quantification of Mfn1 protein levels and H Mfn2 levels, both show no differences between HCS and AD-derived iN cells. I Level of *OPA1* mRNA, assessed by qRT-PCR, was lower in AD2 compared to HCS1 iN cells. J Fission protein Drp1 and phosphorylated-Drp1 levels were assessed by western blot. K Quantification showed no changes between HCS and AD-derived iN cells for total Drp1. L No changes were observed in phosphorylated-Drp1 levels to total Drp1. M Levels of FIS1 mRNA were assessed by RT-qPCR and showed no difference between HCS and AD patient-derived iN cells. Data are means ± SEM (n = 8–12). Statistical significance was assessed one-way ANOVA test (G-I; K-M) or by Kruskal-Wallis test (B-E) (*p < 0.05; **p < 0.01; ***p < 0.001).

abundance of these products were changed in AD-derived iN cells. We detected slightly higher C99/C83 ratios in AD1 to HCS2 cells, other cell lines showed no change in processing ratios (Fig. 4C). Absolute C99 and C83 levels did not differ between control and AD cells (Figs. 4D,E and S4C,D). As further processing of C99 by γ-secretase (De Strooper, 2010) leads to production of different Aβ species, we examined the ratios of Aβ42 to Aβ40 in HCS and AD-patient-derived iN cells. Supernatant of iN cells was conditioned for 7 days and subsequently used for

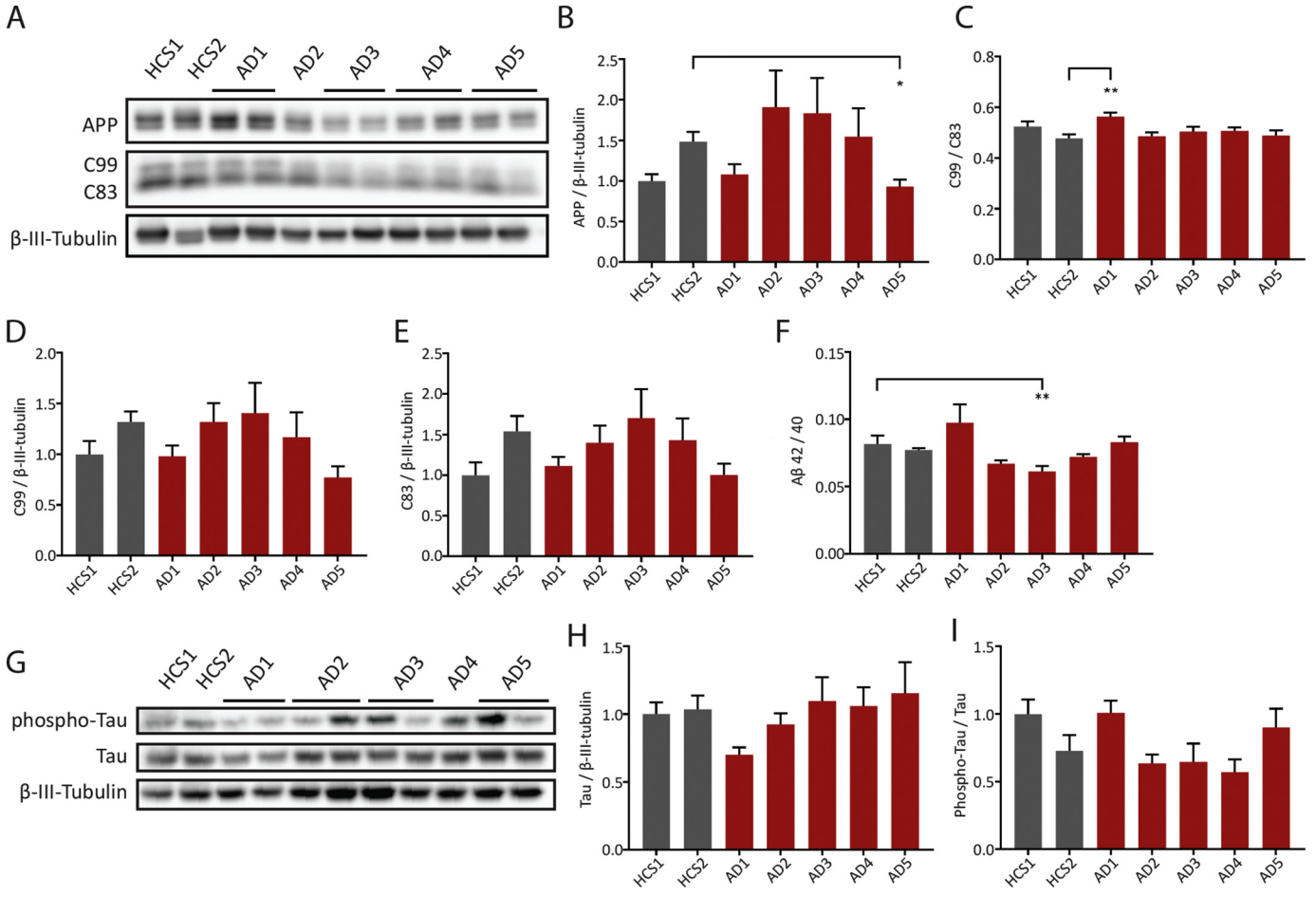

Fig. 4. Characterization of AD hallmark proteins in HCS and AD patient-derived iN cells. A Protein levels of APP and α- and ß-secretase processing products C83 and C99, determined by western-blot. B Quantification of APP levels. HCS2 APP levels were significantly higher compared to AD5. C Quantification of C99 to C83 ratios. Ratio was shifted toward C99 in AD1 compared to HCS2. D,E Quantification of absolute C99 and C83 levels with no difference in AD and HCS-derived cells. n = 12–16; three independent experiments. F Analysis of Aβ42 to Aβ40 secretion of iN cells. Supernatant was conditioned from d21 to d28 and Aβ levels were subsequently measured by MSD. Aβ42 to 40 ratio is lower in AD3 compared to HCS1. G Assessment of total and phosphorylated tau levels by western blot. H Quantification of total tau levels in patient and control-derived iN cells. I Quantification of phosphorylated tau to total tau levels. I,J n = 12–18; Data are means ± SEM. Statistical significance was assessed by Kruskal-Wallis test (*p < 0.05; **p < 0.01).

MSD analysis. Aβ42 is regarded as the most toxic species and its ratio to Aβ40 is an essential determinant of amyloid aggregation in AD (McGowan et al., 2005). MSD analysis showed no difference in Aβ42 to 40 ratios, except for cells from patient AD3, which displayed a lower ratio compared to HCS1 (Fig. 4F). Analysis of absolute Aβ levels showed higher total Aβ40 and 42 in AD5 iN cells compared to HCS2 and lower levels of Aβ40 and Aβ42 in AD3 compared to HCS1 (Fig. S4E,F). Analysis of total and phosphorylated tau by western blot showed no differences between AD and HCS iN cells (Fig. 4G–I and S4G,H). Taken together, APP processing and tau modification are not altered in AD patient iN cells. The increase in total Aβ levels in the AD5 cell lines does not correlate with the findings of ROS formation in AD cells, as AD5 iN cells did not show increased ROS levels.

Oxidative stress and dysregulation of mitochondrial proteins can induce downstream effects, such as DNA damage (Quiros et al., 2016) or synaptic dysfunctions (Kamat et al., 2016). Phosphorylation of histone H2AX has been identified as marker of DNA double-strand breaks (Rogakou et al., 1998). Immunocytochemistry of phosphorylated γ-H2AX in neuronal nuclei, stained by NeuN, revealed slight but significantly higher DNA damage in iN cells from patient AD2 and AD4 compared to HCS2 but not to HCS1 (Fig. S5A,B).

Loss of synapses is the best correlate to the onset of cognitive decline in AD (Terry et al., 1991). We set out to examine levels of different pre- and post-synaptic proteins in HCS and AD-derived iN cells. Levels of synapsin1, a marker of the presynapse, was found to be similar in iN cells from patients and controls (Fig. S6A–C). Analysis of PSD95, a major scaffold in the postsynapse, showed lower levels in AD1 cells compared to HCS2 (Fig. S6D–F). DrebrinA, an actin binding protein involved in recruitment of PSD95 to postsynapses (Takahashi et al., 2003) is downregulated in AD brains (Shim & Lubec, 2002). In line with our previous results, comparison of patient and control lines displayed no significant changes in protein levels (Fig. S6G–I). Taken together, no major synaptic alterations between HCS's and AD patients were found, suggesting that these alterations may depend on Aβ and arise later in the disease (Birnbaum et al., 2015; Palop & Mucke, 2010).

4. Discussion

In this study we examined disease pathology in iPSC-derived neuronal cells from AD patients with a very high diagnostic certainty and healthy control subjects (find summarized results in Table 2). Using a rapid neuronal differentiation protocol we were able to examine pure human neuronal cells, without culture impurities from other human cell types, in contrast to differentiation protocols which were used previously to examine SAD pathology (Kondo et al., 2013; Israel et al., 2012). The use of iN cells allows investigation of early AD, before onset of amyloid and tau pathology. We showed that some patient-derived iN cells display increased ROS production and aberrant mitochondrial complex composition, which did not correlate with Aβ, tau or p-tau levels. Our findings suggest a strong involvement of altered

Table 2
Summary of results comparing individual AD subjects (AD1-5) to HCS1 and HCS2.

	AD1		AD2		AD3		AD4		AD5	
	vs. HCS1	vs HCS2	vs. HCS1	vs HCS2	vs. HCS1	vs HCS2	vs. HCS1	vs HCS2	vs. HCS1	vs HCS2
ROS levels	↔	↔	↑	↑	↑	↑	↑	↑	↔	↔
Complex I protein levels	↔	↔	↔	↔	↔	↔	↑	↑	↔	↔
Complex III protein levels	↔	↔	↔	↔	↔	↔	↑	↔	↑	↔
Complex IV protein levels	↑	↔	↑	↔	↑	↔	↑	↑	↑	↑
Complex V protein levels	↔	↔	↑	↔	↔	↔	↑	↔	↔	↔
Mfn1 protein levels	↔	↔	↔	↔	↔	↔	↔	↔	↔	↔
Mfn2 protein levels	↔	↔	↔	↔	↔	↔	↔	↔	↔	↔
OPA1 mRNA levels	↔	↔	↓	↔	↔	↔	↔	↔	↔	↔
Drp1 protein levels	↔	↔	↔	↔	↔	↔	↔	↔	↔	↔
P-Drp1 protein levels	↔	↔	↔	↔	↔	↔	↔	↔	↔	↔
FIS1 mRNA levels	↔	↔	↔	↔	↔	↔	↔	↔	↔	↔
APP protein levels	↔	↔	↔	↔	↔	↔	↔	↔	↔	↓
Total Aβ 42	↔	↔	↔	↔	↓	↔	↔	↔	↔	↑
Total Aβ 40	↔	↔	↔	↔	↓	↔	↔	↔	↔	↔
Aβ42/40 ratio	↔	↔	↔	↔	↓	↔	↔	↔	↔	↔
Total Tau protein levels	↔	↔	↔	↔	↔	↔	↔	↔	↔	↔
P-Tau protein levels	↔	↔	↔	↔	↔	↔	↔	↔	↔	↔
Synapsin protein levels	↔	↓	↔	↔	↔	↔	↔	↔	↔	↔
PSD95 protein levels	↔	↔	↔	↔	↔	↔	↔	↔	↔	↔
Drebrin protein levels	↔	↔	↔	↔	↔	↔	↔	↔	↔	↔
γ-H2AX intensity	↔	↔	↔	↑	↔	↑	↔	↑	↔	↔

↑: significant increase; ↓: significant decrease; ↔: no significant differences.

mitochondrial function in early AD. Increased ROS levels have been observed in various AD models (Rhein et al., 2009; Reddy et al., 2004; Hauptmann et al., 2009; Hyun et al., 2010) and were found to be implicated in other neurodegenerative processes (Busciglio & Yankner, 1995; Liu et al., 2015; Zhao & Zhao, 2013). ROS production often promotes DNA damage and vice versa (Quiros et al., 2016) and we also observed increased DNA damage in our samples. The relation between ROS and DNA damage is supported by the finding that the AD cell lines with highest ROS levels also showed the highest degree of DNA damage. We further analyzed the composition of the mitochondrial oxidative phosphorylation chain, with complex I and III of the respiratory chain being the main sites of ROS production. We found an upregulation of complex IV subunit MTOC1 in all and upregulations of complex I, III, and V in certain AD-derived iN cells. Cells from patient AD4 showed higher levels of complex I and III, which could explain the increased ROS levels. However, in AD2 and AD3 patient-derived iN cells, which also showed increased ROS production, no changes in these complexes were seen. Thus, ROS production here might be caused by an alternative mechanism, with complex IV upregulation as part of an oxidant defense mechanism (Turrens, 2003). The changes in oxphos protein levels were in line with reports showing an upregulation in complex I, III, IV and V in brains of AD patients (Nagy et al., 1999) and Tg2576 mice (Reddy et al., 2004), whereas contradicting reports found lower levels of cytochrome C oxidase (COX) in complex IV (Bosetti et al., 2002; Perez-Gracia et al., 2008). We argue that our findings of complex IV upregulation may represent compensatory mechanisms, in order to account for reduced functionality. Mitochondrial fission and fusion abnormalities by assessment of MFN1/2, OPA1, DRP1, phosphorylated-DRP1 and FIS1 levels could not be detected in our samples, with the exception of AD2 cells showing lower OPA1 mRNA levels. Previous studies reported reduced OPA1, MFN1, and MFN2 levels and higher FIS1 levels in human AD brain tissue. Drp1 analysis has been reported to be lower in AD tissue in one study and higher levels in another (Wang et al., 2009; Manczak & Reddy, 2012). As we observed a stronger effect on complex dysregulation than changes in fission and fusion, we speculate that these changes in AD brains may arise later in disease and are not visible at an early stage. Examination of APP processing is in line with prior observations that familial AD patients suffer from increased APP levels (APP duplication) or increased Aβ production, whereas sporadic patients mostly have normal APP and Aβ levels (Kondo et al., 2013; Israel et al., 2012). Yet, the strongest risk factor for sporadic AD ApoE4 has recently been linked with higher APP transcription in human stem cell-derived iN cells (Huang et al., 2017). We can rule out ApoE derived effects in our system, as mouse glia, that is used for co-cultures in our system, only produces one ApoE isoform. Abnormal tau phosphorylation has been linked with tangle formation and neurodegeneration (Alonso et al., 1996; Tackenberg & Brandt, 2009; Tackenberg et al., 2013; Goedert et al., 1989). We could not detect changes in tau phosphorylation, whereat it is important to note that iPSC-derived iN cells only express 3R and no 4R tau (unpublished results), which does not reflect the situation in adult neuronal cells (Sposito et al., 2015). We cannot rule out that epigenetic effects might have contributed to AD progression, which cannot be detected in reprogrammed cells (De Jager et al., 2014; Lunnon et al., 2014), or that some of the phenotypes we observed are due to reprogramming induced mutations (Kilpinen et al., n.d.).

We are aware that this study is based on an in vitro system of pure cortical neurons, in which cells are deprived of their physiological microenvironment. This has to be taken into account, especially when results shall be translated to the pathologic processes in patients or even into potential clinical trials. However, this is currently the only technique allowing the analyses of human, patient-derived cells. Further, AD is a complex disease in which also other cell types such as astrocytes and microglia play a crucial role, as well as vascular deficits (Derungs et al., 2017; Paolicelli et al., 2017; Merlini et al., 2016). Systems based on iPSC-derived cells will allow uncovering contributions of different cell types to AD pathogenesis in a controlled fashion. Accordingly, techniques for differentiation of iPSCs into other disease-relevant cell types are currently under extensive research.

We cannot fully exclude that gender differences influenced the results obtain in our analyses. However, the following reasons make this influence unlikely: i) We did not observe effects in all AD patients, i.e. AD1 (female) cells did not differ from HCS1 or HCS2 (both males); ii) Studies on mitochondria of male and female mice did not show differences in bioenergetics, oxidative stress and apoptosis (Sanz et al., 2007); iii) Several iPS studies analyzing APP processing, Aβ production, Tau phosphorylation, oxidative stress, caspase activation, calcium signaling, electrophysiological properties or gene-expression patterns in human neurons did not show gender-related effects, only general inter-individual variations, similar to what we observed in our study (Kondo et al., 2013; Israel et al., 2012; Duan et al., 2014; Hu et al., 2015).

Our study showing oxidative stress and mitochondrial aberrations in iPSC-derived AD patient neuronal cells, which captures an early

phenotype of the disease, raises further questions. A more in depth analysis of mitochondrial changes will be necessary to show if these changes converge at a certain pathway and how this affects energy metabolism, mitochondrial localization and transport, and ultimately neuronal function. Cellular mitochondrial changes might also exert effects on surrounding tissue, creating a local dysregulated environment.

5. Conclusions

Prior studies using iPSC-derived neurons focused on Aβ- and tau-mediated effects in SAD and FAD patient-derived cells (Kondo et al., 2013; Israel et al., 2012). Here we reported increased ROS generation and mitochondrial complex levels in patient-derived iN cells, which does not correlate with Aβ or tau levels. Thus, these AD-relevant mitochondrial aberrations might have a causative role in disease development in early stages preceding amyloid and tau pathology or they might render cells more susceptible for Aβ- and tau-mediated neurodegeneration in later stages of the disease.

Supplementary data to this article can be found online at https://doi.org/10.1016/j.scr.2018.01.019.

Ethics approval

All performed experiments were conducted with the approval and according to the regulations of the Cantonal Ethics Committee and with informed consent of participants. Dermal punch biopsies were taken following informed consent at the Clinic for Dermatology of the University Hospital Zurich.

Competing interests

The authors declare that they have no competing interests.

Funding

This research was supported by grants from the Novartis Foundation for medical-biological research (14C176), the UZH Forschungskredit (FK-15-023), the Olga Mayenfisch Foundation and the Mäxi Foundation.

Author contributions

C.T., R.M.N and J.H.B initiated and R.M.N and C.T. coordinated the project. A.F.G., A.S., T.K. and C.H. were responsible for clinical study design and conduct, ethics approval, patient recruitment, clinical assessments and medical management of skin biopsies (performed by T.K.). J.H.B reprogrammed cells, maintained iPSCs and assessed DNA damage. J.H.B, D.W. and C.T. characterized iPS cells. D.W. and J.H.B differentiated cells, did qRT-PCRs and MSD measurements. J.H.B and D.W. did western blots and analyzed data. J.H.B., D.W. and C.T. did CellRox assays. J.H.B prepared figures, J.H.B and C.T wrote the manuscript.

Acknowledgements

We would like to thank all the study participants that supported this work. Furthermore we like to thank Esmeralda Gruber for providing care during biopsies, Sarina Thöni for karyotyping, and the Institute for Medical Genetics for reagents. Further thanks to Dr. Thomas Südhof and Dr. Christopher Patzke for advice, scientific exchange, reagents and plasmids.

References

Alonso, A.C., Grundke-Iqbal, I., Iqbal, K., 1996. Alzheimer's disease hyperphosphorylated tau sequesters normal tau into tangles of filaments and disassembles microtubules. Nat. Med. 2, 783–787.

Birnbaum, J.H., Bali, J., Rajendran, L., Nitsch, R.M., Tackenberg, C., 2015. Calcium flux-independent NMDA receptor activity is required for Abeta oligomer-induced synaptic loss. Cell Death Dis. 6, e1791.

Bosetti, F., Brizzi, F., Barogi, S., Mancuso, M., Siciliano, G., Tendi, E.A., Murri, L., Rapoport, S. I., Solaini, G., 2002. Cytochrome c oxidase and mitochondrial F1F0-ATPase (ATP synthase) activities in platelets and brain from patients with Alzheimer's disease. Neurobiol. Aging 23, 371–376.

Brownjohn, P.W., Smith, J., Portelius, E., Serneels, L., Kvartsberg, H., De Strooper, B., Blennow, K., Zetterberg, H., Livesey, F.J., 2017. Phenotypic screening identifies modulators of amyloid precursor protein processing in human stem cell models of Alzheimer's disease. Stem Cell Rep. 8, 870–882.

Busciglio, J., Yankner, B.A., 1995. Apoptosis and increased generation of reactive oxygen species in Down's syndrome neurons in vitro. Nature 378, 776–779.

Carpenter, A.E., Jones, T.R., Lamprecht, M.R., Clarke, C., Kang, I.H., Friman, O., Guertin, D.A., Chang, J.H., Lindquist, R.A., Moffat, J., Golland, P., Sabatini, D.M., 2006. CellProfiler: image analysis software for identifying and quantifying cell phenotypes. Genome Biol. 7, R100.

Caspersen, C., Wang, N., Yao, J., Sosunov, A., Chen, X., Lustbader, J.W., Xu, H.W., Stern, D., McKhann, G., Yan, S.D., 2005. Mitochondrial Abeta: a potential focal point for neuronal metabolic dysfunction in Alzheimer's disease. FASEB J. 19, 2040–2041.

Chen, C., Okayama, H., 1987. High-efficiency transformation of mammalian cells by plasmid DNA. Mol. Cell. Biol. 7, 2745–2752.

Chen, G., Gulbranson, D.R., Hou, Z., Bolin, J.M., Ruotti, V., Probasco, M.D., Smuga-Otto, K., Howden, S.E., Diol, N.R., Propson, N.E., Wagner, R., Lee, G.O., Antosiewicz-Bourget, J., Teng, J.M., Thomson, J.A., 2011. Chemically defined conditions for human iPSC derivation and culture. Nat. Methods 8, 424–429.

De Jager, P.L., Srivastava, G., Lunnon, K., Burgess, J., Schalkwyk, L.C., Yu, L., Eaton, M.L., Keenan, B.T., Ernst, J., McCabe, C., Tang, A., Raj, T., Replogle, J., Brodeur, W., Gabriel, S., Chai, H.S., Younkin, C., Younkin, S.G., Zou, F., Szyf, M., Epstein, C.B., Schneider, J.A., Bernstein, B.E., Meissner, A., Ertekin-Taner, N., Chibnik, L.B., Kellis, M., Mill, J., Bennett, D.A., 2014. Alzheimer's disease: early alterations in brain DNA methylation at ANK1, BIN1, RHBDF2 and other loci. Nat. Neurosci. 17, 1156–1163.

De Strooper, B., 2010. Proteases and proteolysis in Alzheimer disease: a multifactorial view on the disease process. Physiol. Rev. 90, 465–494.

Derungs, R., Camici, G.G., Spescha, R.D., Welt, T., Tackenberg, C., Spani, C., Wirth, F., Grimm, A., Eckert, A., Nitsch, R.M., Kulic, L., 2017. Genetic ablation of the p66Shc adaptor protein reverses cognitive deficits and improves mitochondrial function in an APP transgenic mouse model of Alzheimer's disease. Mol. Psychiatry 22, 605–614.

Duan, L., Bhattacharyya, B.J., Belmadani, A., Pan, L., Miller, R.J., Kessler, J.A., 2014. Stem cell derived basal forebrain cholinergic neurons from Alzheimer's disease patients are more susceptible to cell death. Mol. Neurodegener. 9, 3.

DuBoff, B., Feany, M., Gotz, J., 2013. Why size matters - balancing mitochondrial dynamics in Alzheimer's disease. Trends Neurosci. 36, 325–335.

Goedert, M., Spillantini, M.G., Jakes, R., Rutherford, D., Crowther, R.A., 1989. Multiple isoforms of human microtubule-associated protein tau: sequences and localization in neurofibrillary tangles of Alzheimer's disease. Neuron 3, 519–526.

Grimm, A., Friedland, K., Eckert, A., 2016. Mitochondrial dysfunction: the missing link between aging and sporadic Alzheimer's disease. Biogerontology 17, 281–296.

Hauptmann, S., Scherping, I., Drose, S., Brandt, U., Schulz, K.L., Jendrach, M., Leuner, K., Eckert, A., Muller, W.E., 2009. Mitochondrial dysfunction: an early event in Alzheimer pathology accumulates with age in AD transgenic mice. Neurobiol. Aging 30, 1574–1586.

Hirai, K., Aliev, G., Nunomura, A., Fujioka, H., Russell, R.L., Atwood, C.S., Johnson, A.B., Kress, Y., Vinters, H.V., Tabaton, M., Shimohama, S., Cash, A.D., Siedlak, S.L., Harris, P. L., Jones, P.K., Petersen, R.B., Perry, G., Smith, M.A., 2001. Mitochondrial abnormalities in Alzheimer's disease. J. Neurosci. 21, 3017–3023.

Hu, W., Qiu, B., Guan, W., Wang, Q., Wang, M., Li, W., Gao, L., Shen, L., Huang, Y., Xie, G., Zhao, H., Jin, Y., Tang, B., Yu, Y., Zhao, J., Pei, G., 2015. Direct conversion of normal and Alzheimer's disease human fibroblasts into neuronal cells by small molecules. Cell Stem Cell 17, 204–212.

Huang, Y.A., Zhou, B., Wernig, M., Sudhof, T.C., 2017. ApoE2, ApoE3, and ApoE4 differentially stimulate APP transcription and Abeta secretion. Cell 168, 427–441 (e421).

Hyun, D.H., Mughal, M.R., Yang, H., Lee, J.H., Ko, E.J., Hunt, N.D., de Cabo, R., Mattson, M.P., 2010. The plasma membrane redox system is impaired by amyloid beta-peptide and in the hippocampus and cerebral cortex of 3xTgAD mice. Exp. Neurol. 225, 423–429.

Israel, M.A., Yuan, S.H., Bardy, C., Reyna, S.M., Mu, Y., Herrera, C., Hefferan, M.P., Van Gorp, S., Nazor, K.L., Boscolo, F.S., Carson, C.T., Laurent, L.C., Marsala, M., Gage, F.H., Remes, A. M., Koo, E.H., Goldstein, L.S., 2012. Probing sporadic and familial Alzheimer's disease using induced pluripotent stem cells. Nature 482, 216–220.

Kamat, P.K., Kalani, A., Rai, S., Swarnkar, S., Tota, S., Nath, C., Tyagi, N., 2016. Mechanism of oxidative stress and synapse dysfunction in the pathogenesis of Alzheimer's disease: understanding the therapeutics strategies. Mol. Neurobiol. 53, 648–661.

H. Kilpinen, A. Goncalves, A. Leha, V. Afzal, K. Alasoo, S. Ashford, S. Bala, D. Bensaddek, F.P. Casale, O.J. Culley, P. Danecek, A. Faulconbridge, P.W. Harrison, A. Kathuria, D. McCarthy, S.A. McCarthy, R. Meleckyte, Y. Memari, N. Moens, F. Soares, A. Mann, I. Streeter, C.A. Agu, A. Alderton, R. Nelson, S. Harper, M. Patel, A. White, S.R. Patel, L. Clarke, R. Halai, C.M. Kirton, A. Kolb-Kokocinski, P. Beales, E. Birney, D. Danovi, A.I. Lamond, W.H. Ouwehand, L. Vallier, F.M. Watt, R. Durbin, O. Stegle, D.J. Gaffney, Common genetic variation drives molecular heterogeneity in human iPSCs, Nature, 546 (2017) 370–375.

T. Kondo, M. Asai, K. Tsukita, Y. Kutoku, Y. Ohsawa, Y. Sunada, K. Imamura, N. Egawa, N. Yahata, K. Okita, K. Takahashi, I. Asaka, T. Aoi, A. Watanabe, K. Watanabe, C. Kadoya, R. Nakano, D. Watanabe, K. Maruyama, O. Hori, S. Hibino, T. Choshi, T. Nakahata, H. Hioki, T. Kaneko, M. Naitoh, K. Yoshikawa, S. Yamawaki, S. Suzuki, R. Hata, S. Ueno, T. Seki, K. Kobayashi, T. Toda, K. Murakami, K. Irie, W.L. Klein, H. Mori, T. Asada, R. Takahashi, N. Iwata, S. Yamanaka, H. Inoue, Modeling Alzheimer's disease with

iPSCs reveals stress phenotypes associated with intracellular Aβ and differential drug responsiveness., Cell Stem Cell, 12 (2013) 487–496.
Liu, L., Zhang, K., Sandoval, H., Yamamoto, S., Jaiswal, M., Sanz, E., Li, Z., Hui, J., Graham, B. H., Quintana, A., Bellen, H.J., 2015. Glial lipid droplets and ROS induced by mitochondrial defects promote neurodegeneration. Cell 160, 177–190.
Lunnon, K., Smith, R., Hannon, E., De Jager, P.L., Srivastava, G., Volta, M., Troakes, C., Al-Sarraj, S., Burrage, J., Macdonald, R., Condliffe, D., Harries, L.W., Katsel, P., Haroutunian, V., Kaminsky, Z., Joachim, C., Powell, J., Lovestone, S., Bennett, D.A., Schalkwyk, L.C., Mill, J., 2014. Methylomic profiling implicates cortical deregulation of ANK1 in Alzheimer's disease. Nat. Neurosci. 17, 1164–1170.
Manczak, M., Reddy, P.H., 2012. Abnormal interaction between the mitochondrial fission protein Drp1 and hyperphosphorylated tau in Alzheimer's disease neurons: implications for mitochondrial dysfunction and neuronal damage. Hum. Mol. Genet. 21, 2538–2547.
McGowan, E., Pickford, F., Kim, J., Onstead, L., Eriksen, J., Yu, C., Skipper, L., Murphy, M.P., Beard, J., Das, P., Jansen, K., DeLucia, M., Lin, W.L., Dolios, G., Wang, R., Eckman, C.B., Dickson, D.W., Hutton, M., Hardy, J., Golde, T., 2005. Abeta42 is essential for parenchymal and vascular amyloid deposition in mice. Neuron 47, 191–199.
McKhann, G.M., Knopman, D.S., Chertkow, H., Hyman, B.T., Jack Jr., C.R., Kawas, C.H., Klunk, W.E., Koroshetz, W.J., Manly, J.J., Mayeux, R., Mohs, R.C., Morris, J.C., Rossor, M.N., Scheltens, P., Carrillo, M.C., Thies, B., Weintraub, S., Phelps, C.H., 2011. The diagnosis of dementia due to Alzheimer's disease: recommendations from the National Institute on Aging-Alzheimer's Association workgroups on diagnostic guidelines for Alzheimer's disease. Alzheimers Dement. 7, 263–269.
Mecocci, P., MacGarvey, U., Beal, M.F., 1994. Oxidative damage to mitochondrial DNA is increased in Alzheimer's disease. Ann. Neurol. 36, 747–751.
Merlini, M., Wanner, D., Nitsch, R.M., 2016. Tau pathology-dependent remodelling of cerebral arteries precedes Alzheimer's disease-related microvascular cerebral amyloid angiopathy. Acta Neuropathol. 131, 737–752.
Mertens, J., Stüber, K., Wunderlich, P., Ladewig, J., Kesavan, J., Vandenberghe, R., Vandenbulcke, M., van Damme, P., Walter, J., Brüstle, O., Koch, P., 2013. APP processing in human pluripotent stem cell-derived neurons is resistant to NSAID-based γ-secretase modulation. Stem Cell Reports 1, 491–498.
Moore, S., Evans, L.D., Andersson, T., Portelius, E., Smith, J., Dias, T.B., Saurat, N., McGlade, A., Kirwan, P., Blennow, K., Hardy, J., Zetterberg, H., Livesey, F.J., 2015. APP metabolism regulates tau proteostasis in human cerebral cortex neurons. Cell Rep. 11, 689–696.
Nagy, Z., Esiri, M.M., LeGris, M., Matthews, P.M., 1999. Mitochondrial enzyme expression in the hippocampus in relation to Alzheimer-type pathology. Acta Neuropathol. 97, 346–354.
Nicolas, G., Charbonnier, C., Campion, D., 2016. From common to rare variants: the genetic component of Alzheimer disease. Hum. Hered. 81, 129–141.
Okita, K., Matsumura, Y., Sato, Y., Okada, A., Morizane, A., Okamoto, S., Hong, H., Nakagawa, M., Tanabe, K., Tezuka, K., Shibata, T., Kunisada, T., Takahashi, M., Takahashi, J., Saji, H., Yamanaka, S., 2011. A more efficient method to generate integration-free human iPS cells. Nat. Methods 8, 409–412.
Palop, J.J., Mucke, L., 2010. Amyloid-beta-induced neuronal dysfunction in Alzheimer's disease: from synapses toward neural networks. Nat. Neurosci. 13, 812–818.
Paolicelli, R.C., Jawaid, A., Henstridge, C.M., Valeri, A., Merlini, M., Robinson, J.L., Lee, E.B., Rose, J., Appel, S., Lee, V.M., Trojanowski, J.Q., Spires-Jones, T., Schulz, P.E., Rajendran, L., 2017. TDP-43 depletion in microglia promotes amyloid clearance but also induces synapse loss. Neuron 95 297–308.e296.
Perez-Gracia, E., Torrejon-Escribano, B., Ferrer, I., 2008. Dystrophic neurites of senile plaques in Alzheimer's disease are deficient in cytochrome c oxidase. Acta Neuropathol. 116, 261–268.
Quiros, P.M., Mottis, A., Auwerx, J., 2016. Mitonuclear communication in homeostasis and stress. Nat. Rev. Mol. Cell Biol. 17, 213–226.
Reddy, P.H., McWeeney, S., Park, B.S., Manczak, M., Gutala, R.V., Partovi, D., Jung, Y., Yau, V., Searles, R., Mori, M., Quinn, J., 2004. Gene expression profiles of transcripts in amyloid precursor protein transgenic mice: up-regulation of mitochondrial metabolism and apoptotic genes is an early cellular change in Alzheimer's disease. Hum. Mol. Genet. 13, 1225–1240.
Rhein, V., Song, X., Wiesner, A., Ittner, L.M., Baysang, G., Meier, F., Ozmen, L., Bluethmann, H., Drose, S., Brandt, U., Savaskan, E., Czech, C., Gotz, J., Eckert, A., 2009. Amyloid-beta and tau synergistically impair the oxidative phosphorylation system in triple transgenic Alzheimer's disease mice. Proc. Natl. Acad. Sci. U. S. A. 106, 20057–20062.
Rogakou, E.P., Pilch, D.R., Orr, A.H., Ivanova, V.S., Bonner, W.M., 1998. DNA double-stranded breaks induce histone H2AX phosphorylation on serine 139. J. Biol. Chem. 273, 5858–5868.
Saito, T., Matsuba, Y., Mihira, N., Takano, J., Nilsson, P., Itohara, S., Iwata, N., Saido, T.C., 2014. Single App knock-in mouse models of Alzheimer's disease. Nat. Neurosci. 17, 661–663.
Saito, T., Matsuba, Y., Yamazaki, N., Hashimoto, S., Saido, T.C., 2016. Calpain activation in Alzheimer's model mice is an artifact of APP and presenilin overexpression. J. Neurosci. 36, 9933–9936.
Sanz, A., Hiona, A., Kujoth, G.C., Seo, A.Y., Hofer, T., Kouwenhoven, E., Kalani, R., Prolla, T.A., Barja, G., Leeuwenburgh, C., 2007. Evaluation of sex differences on mitochondrial bioenergetics and apoptosis in mice. Exp. Gerontol. 42, 173–182.
Shim, K.S., Lubec, G., 2002. Drebrin, a dendritic spine protein, is manifold decreased in brains of patients with Alzheimer's disease and down syndrome. Neurosci. Lett. 324, 209–212.
Sposito, T., Preza, E., Mahoney, C.J., Seto-Salvia, N., Ryan, N.S., Morris, H.R., Arber, C., Devine, M.J., Houlden, H., Warner, T.T., Bushell, T.J., Zagnoni, M., Kunath, T., Livesey, F.J., Fox, N.C., Rossor, M.N., Hardy, J., Wray, S., 2015. Developmental regulation of tau splicing is disrupted in stem cell-derived neurons from frontotemporal dementia patients with the 10 + 16 splice-site mutation in MAPT. Hum. Mol. Genet. 24, 5260–5269.
Tackenberg, C., Brandt, R., 2009. Divergent pathways mediate spine alterations and cell death induced by amyloid-beta, wild-type tau, and R406W tau. J. Neurosci. 29, 14439–14450.
Tackenberg, C., Grinschgl, S., Trutzel, A., Santuccione, A.C., Frey, M.C., Konietzko, U., Grimm, J., Brandt, R., Nitsch, R.M., 2013. NMDA receptor subunit composition determines beta-amyloid-induced neurodegeneration and synaptic loss. Cell Death Dis. 4, e608.
Takahashi, H., Sekino, Y., Tanaka, S., Mizui, T., Kishi, S., Shirao, T., 2003. Drebrin-dependent actin clustering in dendritic filopodia governs synaptic targeting of postsynaptic density-95 and dendritic spine morphogenesis. J. Neurosci. 23, 6586–6595.
Takahashi, K., Tanabe, K., Ohnuki, M., Narita, M., Ichisaka, T., Tomoda, K., Yamanaka, S., 2007. Induction of pluripotent stem cells from adult human fibroblasts by defined factors. Cell 131, 861–872.
Terry, R.D., Masliah, E., Salmon, D.P., Butters, N., DeTeresa, R., Hill, R., Hansen, L.A., Katzman, R., 1991. Physical basis of cognitive alterations in Alzheimer's disease: synapse loss is the major correlate of cognitive impairment. Ann. Neurol. 30, 572–580.
Trushina, E., Nemutlu, E., Zhang, S., Christensen, T., Camp, J., Mesa, J., Siddiqui, A., Tamura, Y., Sesaki, H., Wengenack, T.M., Dzeja, P.P., Poduslo, J.F., 2012. Defects in mitochondrial dynamics and metabolomic signatures of evolving energetic stress in mouse models of familial Alzheimer's disease. PLoS One 7, e32737.
Turrens, J.F., 2003. Mitochondrial formation of reactive oxygen species. J. Physiol. 552, 335–344.
Wang, X., Su, B., Lee, H.G., Li, X., Perry, G., Smith, M.A., Zhu, X., 2009. Impaired balance of mitochondrial fission and fusion in Alzheimer's disease. J. Neurosci. 29, 9090–9103.
Winblad, B., Amouyel, P., Andrieu, S., Ballard, C., Brayne, C., Brodaty, H., Cedazo-Minguez, A., Dubois, B., Edvardsson, D., Feldman, H., Fratiglioni, L., Frisoni, G.B., Gauthier, S., Georges, J., Graff, C., Iqbal, K., Jessen, F., Johansson, G., Jonsson, L., Kivipelto, M., Knapp, M., Mangialasche, F., Melis, R., Nordberg, A., Rikkert, M.O., Qiu, C., Sakmar, T. P., Scheltens, P., Schneider, L.S., Sperling, R., Tjernberg, L.O., Waldemar, G., Wimo, A., Zetterberg, H., 2016. Defeating Alzheimer's disease and other dementias: a priority for European science and society. Lancet Neurol. 15, 455–532.
Woodruff, G., Young, J.E., Martinez, F.J., Buen, F., Gore, A., Kinaga, J., Li, Z., Yuan, S.H., Zhang, K., Goldstein, L.S., 2013. The Presenilin-1 ΔE9 mutation results in reduced γ-secretase activity, but not total loss of PS1 function, in isogenic human stem cells. Cell Rep. 5, 974–985.
Yagi, T., Ito, D., Okada, Y., Akamatsu, W., Nihei, Y., Yoshizaki, T., Yamanaka, S., Okano, H., Suzuki, N., 2011. Modeling familial Alzheimer's disease with induced pluripotent stem cells. Hum. Mol. Genet. 20, 4530–4539.
Yao, J., Irwin, R.W., Zhao, L., Nilsen, J., Hamilton, R.T., Brinton, R.D., 2009. Mitochondrial bioenergetic deficit precedes Alzheimer's pathology in female mouse model of Alzheimer's disease. Proc. Natl. Acad. Sci. U. S. A. 106, 14670–14675.
Zhang, Y., Pak, C., Han, Y., Ahlenius, H., Zhang, Z., Chanda, S., Marro, S., Patzke, C., Acuna, C., Covy, J., Xu, W., Yang, N., Danko, T., Chen, L., Wernig, M., Südhof, T.C., 2013. Rapid single-step induction of functional neurons from human pluripotent stem cells. Neuron 78, 785–798.
Zhao, Y., Zhao, B., 2013. Oxidative stress and the pathogenesis of Alzheimer's disease. Oxidative Med. Cell. Longev. 2013, 316523.